

NASA TT F-10,179

SUPERSONIC FLOW AROUND ELLIPSOIDS

A. P. Shvets

FACILITY FORM 602	N66 24925	
	(ACCESSION NUMBER)	(THRU)
	12	1
	(PAGES)	(CODE)
	(NASA CR OR TMX OR AD NUMBER)	(CATEGORY)
		01

Translation of "Obtekaniye ellipsoidov sverkhzvukovym potokom."
Izvestiya Akademii Nauk SSSR. Mekhanika i Mashinostroyeniye,
No. 4. nn. 29-32 1961

GPO PRICE \$ _____

CFSTI PRICE(S) \$ _____

Hard copy (HC) 1.00Microfiche (MF) .50

ff 853 July 85

NATIONAL AERONAUTICS AND SPACE ADMINISTRATION
WASHINGTON MAY 1966

SUPERSONIC FLOW AROUND ELLIPSOIDS

Experimental investigations of supersonic flow around ellipsoidal models and the position of the detached shock waves are described.

Tests were conducted in an intermittent wind tunnel at Mach numbers $M = 1.48, 2.01, 2.53, 3.02$. The Reynolds numbers, referred to 0.1 m length and calculated from the free stream parameters, ranged from $2.0 \cdot 10^6$ to $2.5 \cdot 10^6$. The test models were oblate ellipsoids of revolution with semi-axis ratios $t = b/a = 0.49, 0.34, \text{ and } 0.19$. Each model had 11 pressure orifices situated symmetrically about the axis. The pressure distribution on the surface of the ellipsoid with semi-axis ratio $t = 0.34$ is shown in figure 1 for $M = 3.02$ (the cross section $\Psi = 0 - 180^\circ$). The experimental points for angles of attack $\alpha = 0, 5, 10, \text{ and } 15^\circ$ are joined by solid curves. The dashed curves in figure 1 give the values of c_p/c_{p0} for $\alpha = 0, 5, 10^\circ$, calculated according to the refined Newtonian equation

$$c_p = \frac{c_{p0}}{\sin^2 \alpha_0} \frac{(\cos \alpha \sqrt{1-r^2} - rt \sin \alpha \cos \psi)^2}{1+r^2(t^2-1)} \quad (1)$$

where c_{p0} is the value given by the theory of supersonic flow of an ideal gas for the pressure coefficient at the leading apex of the body, α_0 is the angle between the tangent to the body contour at this point and the free stream centerline, $r = R/a$ is the dimensionless radius. It is necessarily pointed out that equation (1) does not enable one to find the pressure on portions of the body in its "aerodynamic shadow." According to Newtonian theory, the pressure on these areas of the surface is equal to zero.

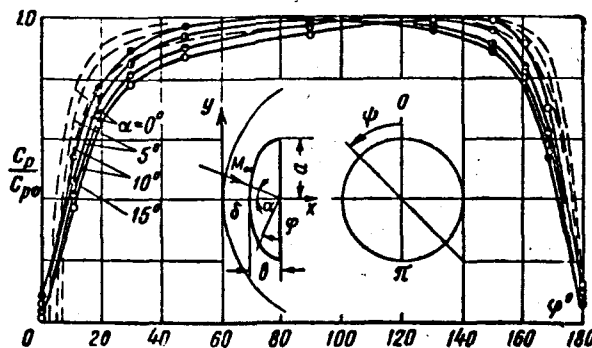


Figure 1

*Numbers in the margin indicate pagination in the original foreign text.

The tangential and normal force coefficients of the ellipsoids are equal to

$$c_\tau = \frac{1}{\frac{1}{2}\gamma p_\infty M^2 \pi a^3} \int_0^{2\pi} \int_0^\pi (p_a - p_\infty) R dR d\psi$$

$$c_n = -\frac{1}{\frac{1}{2}\gamma p_\infty M^2 \pi a^3} \int_0^{2\pi} \int_0^\pi (p_a - p_\infty) R \operatorname{tg} \beta \cos \psi dR d\psi$$

Here p_∞ , M are the pressure and free stream Mach number, γ is the adiabatic exponent, p_a is the absolute pressure on the surface of the body, β is the angle between the normal to the surface and the axis of the body.

In calculating the aerodynamic performance curves of the ellipsoids in supersonic flow at various angles of attack, the assumption was made that

/30

$$p(r\psi) = p_+(r) + p_-(r) \cos \psi \quad (2)$$

Here

$$p_+(r) = \frac{1}{2}[p(r0) + p(r\pi)]$$

$$p_-(r) = \frac{1}{2}[p(r0) - p(r\pi)]$$

$$p = \frac{P_a - P_\infty}{P_0'}$$

The quantity p_0' denotes the total pressure directly behind the discontinuity.

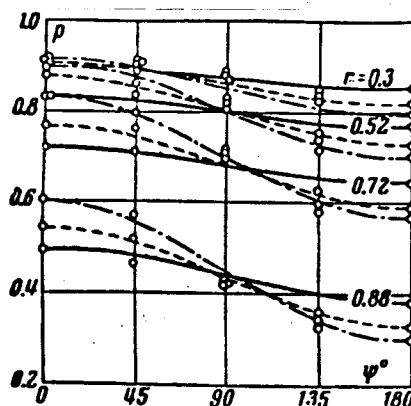


Figure 2

The pressure on the ellipsoid ($t = 0.34$) is shown in figure 2 as a function of the angle Ψ for $M = 3.02$ and streaming at oblique angles of attack. The experimental values of p for fixed values of the dimensionless radius are compared with the values calculated from equation (2). The curves calculated according to equation (2) are represented in figure 2 by solid curves for $\alpha = 5^\circ$, by dashed curves for $\alpha = 10^\circ$, and by dot-dash curves for $\alpha = 15^\circ$. It is apparent from inspection of the graph that the experimental distribution of pressure with respect to the angle Ψ is satisfactorily approximated by a cosine

curve. This makes it possible to carry out an approximate calculation of the aerodynamic performance curves for the ellipsoids on the basis of data on the pressure distribution over the contour of one section of the model in the plane of the angle of attack, thus, reducing the computational effort. The tangential force coefficient, taking the assumption (2) into account, acquires the form

$$c_\tau = \frac{4p_0'}{\gamma P_\infty M^2} \int_0^1 p_+(r) r dr$$

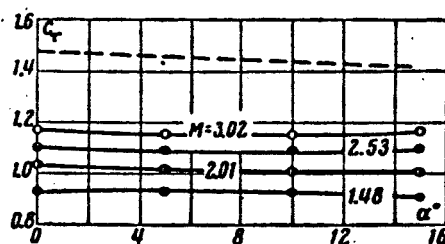


Figure 3

The graph of figure 3 shows the variation of the tangential force coefficient for the ellipsoid with semi-axis ratio $t = 0.34$. Each curve was constructed for a definite M number. It is evident from the results of the experiment that in the investigated range of attack angles, $\alpha = 0 \pm 15^\circ$, the tangential force coefficient remains essentially constant ($\pm 4\%$). The dashed line in figure 3 is calculated from equation (1). The analytic curve is about 20% higher than the experimental results for $M = 3.02$.

The tested ellipsoids occupy an intermediate status between a sphere ($t = 1$) and a cylinder with a flat leading part ($t = 0$). It is apparent from figure 4 that flattening of the ellipsoid from $t = 0.49$ to 0.19 increases the wave drag by 15 to 18%; as the M number is increased from 1.48 to 3.02 the tangential force coefficient for all models tested increases by 20 to 22%; the dashed line gives the values of c_τ according to the refined Newtonian equation.

Results of experimental investigations on supersonic flow past plates and bodies of revolution with elliptical frontal portions are described by Holder and Chinneck (ref. 1). The authors obtained data on the pressure distribution, drag, and flow spectra of the models with M numbers ranging from 1.42 to 1.82. The crosses in figure 4 indicate these results for the case of a body of revolution with a flat leading portion, an ellipsoid with semi-axis ratio $t = 0.5$, and a sphere, with $M = 1.42$.

The normal force coefficient is determined from the equation

$$c_n = - \frac{2p_0'}{\gamma P_\infty M^2} \int_0^1 p_-(r) \lg \beta r dr$$

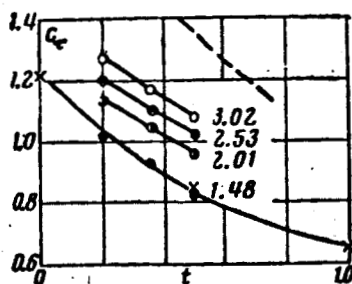


Figure 4

The dependence of the normal force coefficient on the angle of attack is shown in figure 5 for an ellipsoidal model with $t = 0.34$. The solid line joins the experimental points, the dashed line gives the value of C_n calculated from equation (1). In the investigated range of attack angles, $\alpha = 0$ to 15° , the normal force coefficient of the ellipsoids increases linearly with angle of attack.

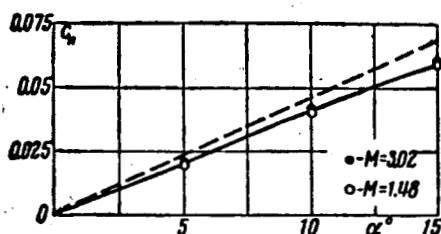


Figure 5

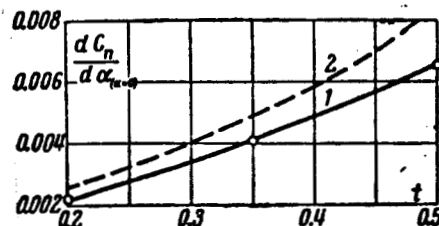


Figure 6

The effect of flattening of the ellipsoid on the value of $dC_n/d\alpha(\alpha=0)$ is shown in figure 6. The experimental data for $M = 3.02$ (curve 1) are compared with the values calculated from the refined Newtonian formula (curve 2).

The shape of the bow wave and stand-off distance were analyzed from photographs of the flow past the ellipsoids at zero angle of attack. Data on the shape and position of the bow wave for the ellipsoid with semi-axis ratio $t = 0.49$ are illustrated in figure 7. The graphs were constructed in the dimensionless coordinates of points on the wave. The numerals 1, 2, 3, 4 refer to the shapes of the head wave and positions of the ellipsoid nose for Mach numbers $M = 3.02, 2.53, 2.01$, and 1.48 , respectively (solid curves). For comparison with the results of the tests at $M = 1.48$, data from reference 1 for a similar ellipsoid with $t = 0.5$ and $M = 1.42$ are also given in figure 7 (dashed curves).

The complex flow behind the shock wave was calculated on electronic computers by numerical methods. Using A. A. Dorodnitsyn's method of integral relations (ref.2), O. M. Belotserkovskiy (ref.3) computed the flow field about the nose sections of ellipsoids of revolution. The dot-dash curve in figure 7 reveals the shape of the head wave for an ellipsoid with semi-axis ratio

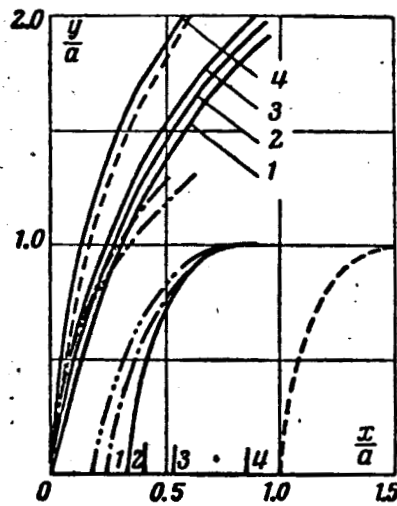


Figure 7

$t = 0.666$ at $M = 4.0$ (ref. 3). In this same figure, the dot-dot-dash curve represents the results of Osborne and Crane's experiments (ref. 4) for an ellipsoid with $t = 0.707$. The flow around models of three axially symmetrical bodies (hemisphere, hyperboloid, and ellipsoid) at $M = 6.8$ was studied in reference 4.

Theoretical and experimental data on the detachment of a compression shock from a body as a function of the free stream Mach number are shown in figure 8. The M number is plotted on the horizontal axis, the ratio δ/a on the vertical axis (where δ is the distance between the shock and the body along the x axis). On the basis of data from the tests described herein, for $M = 1.48, 2.01, 2.53$, and 3.02 (open circles) the curves of $\delta/a = f(M)$ were constructed for ellipsoids with semi-axis ratios $t = 0.19, 0.34$, and 0.49 .

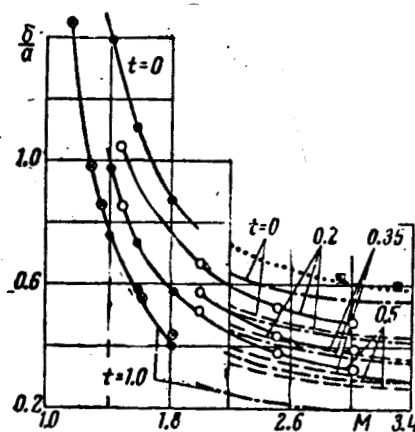


Figure 8

Vinokur (ref. 5) gives two approximate analytical solutions for a family of oblate ellipsoids with constant density. It is assumed, in the first solution,

that the surface of pressure discontinuity is confocal with the surface of the body. In the second solution, the assumption is that the curvature of the discontinuity is constant near the axis. The theoretical data of Vinokur for the parameter δ/a are represented in figure 8 by a dashed curve for the first solution and by a dot-dash curve for the second. The second solution comes nearer the experimental data than the first, although, both gives values for δ/a that are too low relative to the experimental values.

In reference 1, the shock stand-off distance was measured for a cylinder with a flat frontal portion, an ellipsoid, and a sphere for $M = 1.42, 1.6, 1.82$ (heavy dots in figure 8). As is apparent from the graph, the data of reference 1 for an ellipsoid with $t = 0.5$ agrees satisfactorily with the results of our own measurements. As the parameter t is varied from 0.19 to 0.49, the stand-off distance of the shock wave from the ellipsoid (δ/a) decreases from 1.05 to 0.86 for $M = 1.48$, and from 0.48 to 0.33 for $M = 3.02$. Figure 8, also, shows Servin's (ref. 6-7) theoretical (dotted curve) and experimental (squares) values of the parameter δ/a for the case of a flat-ended cylinder, as well as, the results of experiments (ref. 8) on a sphere (circled crosses).

Received 30 March 1964

REFERENCES

1. Holder, D. and A. Chinneck. Observations of the Flow Past Elliptic-Nosed Two-Dimensional Cylinders and Bodies of Revolution in Supersonic Air Streams. Aeron. Quart., Vol. 4, Part 4, 1954.
2. Dorodnitsyn, A. A. A Method for the Numerical Solution of Certain Problems in Aerodynamics (Ob odnom metode chislennogo resheniya nekotorykh aerodinamiki). Transactions of the Third All-Union Mathematics Conference (Trudy III Vsesoyuzn. matem. s"ezda), Vol. 2, 1958.
3. Belotserkovskiy, O. M. Calculation of the Flow Past Axially Symmetrical Bodies with a Detached Shock Wave (Raschet obtekaniya osesimmetrichnykh tel s otoshedshey udarnoy volnoy). Izd. An SSSR, 1961.
4. Osborne, W. K. and J. F. W. Crane. Flow Field and Pressure Distribution Measurements on Blunt-Nosed Bodies at $M = 6.8$. Aeron. Res. Council, Current Paper No. 615, 1962.
5. Vinokur, M. Hypersonic Flow Around Bodies of Revolution Which Are Generated by Conic Sections. Sixth Midwestern Conference on Fluid Mechanics, 1959.
6. Serbin, H. Supersonic Flow Around Blunt Bodies. J. Aeron. Sci., Readers Forum, Vol. 25, No. 1, 1958. The High Speed Flow of Gas Around Blunt Bodies. Aeron. Quart., Vol. 9, Part 4, 1958.
7. Serbin, H. Hypersonic Non-Viscous Flow Around a Circular Disk Normal to the Stream. The RAND Corporation, Research Memorandum RM-1713, May 1956.
8. Heberle, J., Wood, G. and P. Gooderum. Nat. Advisory Comm. Aeron., Technical Note No. 2000, 1950.